

A Model for Perimeter-Defense Problems with Heterogeneous Teams

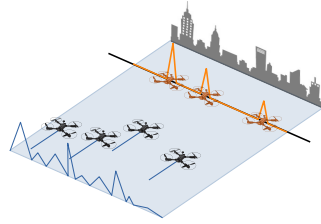
Christopher D. Hsu^{1,2}, Mulugeta A. Haile¹, and Pratik Chaudhari²

Abstract—We develop a model of the multi-agent perimeter-defense game to calculate how an adaptive defense should be organized. This model is inspired by the human immune system and captures settings such as heterogeneous teams, limited resource allocations, partial observability of the attacking side, and decentralization. An optimal defense, that minimizes the harm under constraints of the energy spent to maintain a large and diverse repertoire, must maintain coverage of the perimeter from a diverse attacker population. The model characterizes how a defense might take advantage of its ability to respond strongly to attackers of the same type but weakly to attackers of diverse types to minimize the number of diverse defenders and while reducing harm. We first study the model from a steady-state perimeter-defense perspective and then extend it to mobile defenders and evolving attacker distributions. The optimal defender distribution is supported on a discrete set and similarly a Kalman filter obtaining local information is able to track a discrete, sometimes unknown, attacker distribution. Simulation experiments are performed to study the efficacy of the model under different constraints.

I. INTRODUCTION

Consider two teams, denoted by “defenders” (orange) and “attackers” (blue), each with a heterogeneous group of agents that have different capabilities, say offensive or defensive skills, or mobility. The defenders seek to protect an area against the attacking team which tries to penetrate this defense. The goal of this paper is to understand control policies for the defenders that take into account the heterogeneous nature of this problem.

We draw inspiration from the adaptive immune system which faces a similar problem while protecting an organism from pathogens¹. Some pathogens are persistent but benign (e.g., common cold) and others are rare but dangerous (e.g., HIV). There is a vast number of other pathogens on this spectrum. Tackling every pathogen optimally requires a specialized receptor (these are proteins expressed by lymphocytes whose molecules bind to the molecular constitution of pathogens). It would intuitively seem that the distribution of such receptors should be identical to the distribution of pathogens in the environment. But such a diverse repertoire would come at a large metabolic cost of maintaining all these receptors.



The immune system builds a rather non-intuitive repertoire: it devotes relatively more resources to fighting pathogens that cause large harm even if they are rare and relatively fewer resources to pathogens which cause less harm even if they are encountered frequently. Such a composition seems counter-intuitive. There are two key reasons which lead to its emergence. First, a constraint on the metabolic energy spent on maintaining a large receptor repertoire limits the total number of diverse receptors. And second, there exist specialized receptors that detect and tackle a specific pathogen with high probability but these receptors can also respond to other similar pathogens with a smaller probability and thereby reduce the overall harm to the organism. This paper embodies these ideas into control policies for the defender team.

A. Contributions

We use a theoretical model of the immune system¹ to understand perimeter-defense problems with heterogeneous teams of multiple agents. The defender team seeks to select the appropriate type of agents and an appropriate number of them to minimize the harm caused by a heterogeneous attacker team. We seek to understand two situations: (i) when no single defender can defend against every type of attacker, and (ii) when defenders have limited resources that they should devote optimally to tackle the attackers.

We develop a technique to estimate an unknown attacker distribution. Defenders may not always have full knowledge of the attacker distribution. In this situation, it may be possible to use the information from defender-attacker encounters in a Bayesian filter to estimate the attacker distribution and adapt the defender distribution accordingly. We consider two situations: (i) when the attacker distribution is stationary and does not change over time, and (ii) when it evolves over time.

We show that the defender team can achieve near-optimal harm using a decentralized approach. Centralized computation may seem necessary to select the optimal defender distribution because both local and global structure of the attacker distribution determines it. We study decentralized dynamics where competition between defenders for successful interaction with attackers acts as a reward to encourage the congregation of specific defender types. We show how such local computation leads to near-optimal defender distributions, both when the attacker distribution is stationary, and when it evolves over time. We also study the “centralized estimation and decentralized control” setting where information obtained from individual interactions with the attackers is shared

¹DEVCOM Army Research Laboratory christopher.d.hsu.civ@army.mil, mulugeta.a.haile.civ@army.mil

²Department of Electrical & Systems Engineering and the GRASP Laboratory at the University of Pennsylvania. chs8@seas.upenn.edu, pratikac@seas.upenn.edu

with all the defenders but the competitive dynamics of the defenders is decentralized.

B. Organization

We first formulate the model in §II. We investigate the model under different scenarios using theory and simulation experiments in §§III–VI. We discuss related work in §VII.

II. PROBLEM FORMULATION

Let Q_a be the probability that denotes the next intrusion will be caused by an attacker of type a . Let P_d be the probability of a defender of type d being present. We wish to compute the optimal distribution of the defenders P_d^* that minimizes the harm caused by this intrusion. In biology, attackers a and defenders d interact in an abstract state-space called the shape-space².

In this paper, we will be deliberately vague about what the state-space is. For studying steady-state situations when there is a large number of attackers and defenders, we will think of the shape space as the types of agents (a defender of type d interacts with an attacker of type a); for studying situations when defenders or attackers are mobile, we will think of the shape space as the Euclidean state-space (a, d are locations of agents).

a) Interaction between attackers and defenders: Let us first model the situation when defenders are stationary on/inside the perimeter and get observations from the attackers when both are within a certain distance of each other. We will use a cross-reactivity term $f_{d,a}$ to denote the probability that defender d tackles an attacker a successfully. While the cross-reactivity can be any kernel, we will focus on a Gaussian $f_{d,a} \propto \exp\left(-\frac{(d-a)^2}{2\sigma^2}\right)$ where σ denotes the bandwidth (as mentioned above, σ can refer to the different types of agents, or Euclidean locations). Far away defenders under this kernel have a smaller chance of tackling attackers. The total probability of tackling an attacker a successfully is $\tilde{P}_a = \sum_d f_{d,a} P_d$.

We can model the interaction between an attacker a and some defender d as a Poisson random variable with rate $\lambda_a(t)$. Larger the number of attackers, larger the rate of interaction with them; we model this as a rate that increases exponentially with time $\dot{\lambda}_a(t) = \lambda_a \nu'_a$ starting from some initial rate $\lambda_a(0) = 1$ (for sampled $a \sim Q_a$). In biology, this is because the population of pathogens grows. For us it is because the attacker spends more time in the environment. The expected number of interactions of an attacker with some defender is $m_a(t) = \int_0^t d\tau \lambda_a(\tau) \approx \lambda_a(0)(e^{\nu'_a t} - 1)/\nu'_a$.

b) Harm caused by an attacker: The number of attackers of a type a denoted by $m_a(t)$ also grows exponentially $\dot{m}_a(t) = m_a \nu_a$ starting from some $m_a(0) = 1$ (for sampled $a \sim Q_a$) if it is not tackled successfully. The exponents ν_a and ν'_a may be different because the number of attackers a that cause harm may grow differently than the number of attackers a that can be observed by the defense. Unsuccessful interactions of defenders with attackers cause one unit of

harm. For large times $t \approx \log(m_a/\lambda_a(0))/\nu'_a$, the expected harm caused by an attacker of type a after m unsuccessful interactions is

$$F_a(m) = F_a(0) \left(\frac{m}{\lambda_a(0)} \right)^{\nu_a/\nu'_a} \propto m^\alpha; \quad (1)$$

where $\alpha = \nu_a/\nu'_a$. The quantity $F_a(m)$ is polynomial in the number of interactions m in this paper but it can also take other forms, e.g., $F_a(m) = 1 - e^{-\beta m}$ would model the situation where the harm plateaus after a large number of interactions. The harm \bar{F}_a caused by an attacker a is thus the average recognition time

$$\bar{F}_a = \tilde{P}_a \int_0^\infty dm F_a(m) e^{-m \tilde{P}_a}. \quad (2)$$

We call this the “empirical harm” because we will be able to estimate it using simulations.

c) Minimizing the harm: The harm caused by an attacker sampled from Q_a is

$$\text{Harm}(P_d) = \sum_a Q_a \bar{F}_a. \quad (3)$$

It is a function of the defender distribution P_d and our goal will be to minimize it. When $F_a(m) = m^\alpha$, the optimization problem can be solved analytically to obtain the mean harm

$$\bar{F}_a = \frac{\Gamma(1 + \alpha)}{\tilde{P}_a^\alpha}, \quad (4)$$

where Γ is the Gamma function; see the Appendix. We will refer to this as the “analytical harm” in the rest of the paper. The harm incurred for different settings, e.g., a sub-optimal defender distribution P_d , can be compared to this quantity.

III. OPTIMAL DEFENDER DISTRIBUTION IS SUPPORTED ON A DISCRETE SET

Our cross-reactivity term models the fact that in biology, a given receptor can bind to different pathogens to varying degrees: a non-zero bandwidth σ allows the organism to reduce the number of different types of defenders that it needs to maintain to tackle typical attackers. For a Gaussian $Q_a \propto e^{-a^2/(2\sigma_Q^2)}$,¹ shows that when the cross-reactivity bandwidth σ is smaller than a threshold $\sigma_Q \sqrt{1 + \alpha}$, the optimal defender distribution is also Gaussian

$$P_d^* \propto e^{-\frac{d^2}{2((1+\alpha)\sigma_Q^2 - \sigma^2)}}.$$

Note that the variance is negative if $\sigma/\sigma_Q > \sqrt{1 + \alpha}$. So if the bandwidth is above this threshold, the optimal defense is a Dirac delta at the origin. This shows that cross-reactivity allows concentrated distributions and reduces the need to maintain a diverse number of defenders. We can also show this mathematically where we can turn the variational problem in (3) into a standard optimization problem by assuming a parametric form for the defender distribution $P_d = e^{-d^2/(2\sigma_P^2)}$ (by symmetry it has to be centered at $d = 0$). For a Gaussian Q_a , we can now minimize the harm in (3), to see that the solution has $\sigma_P = 0$.

Such discreteness is also seen in many other problems, e.g., capacity of a Gaussian channel under an amplitude constraint³ and representations in the brain⁴. A somewhat related phenomenon can also be found in the statistics literature which studies priors that are supported over a discrete set⁵. In intuitive terms, a discrete prior (or a discrete defender distribution) allows capturing large parts of the data space (or the attacker distribution) with few resources (models or receptors). These ideas have been studied in information theory⁶ and have also been used to build new methods to learn from unlabeled data in the machine learning literature⁷. In our case, the optimal defender distribution P_d^* also puts its probability mass on diverse types of defenders to best tackle the attackers using the cross-reactivity. Larger the cross-reactivity bandwidth σ , more the spacing in between the atoms of P_d^* . Although, we have argued discreteness in the setting when Q_a is Gaussian, this result is expected to hold in general; see the numerical simulation in Fig. 1.

A. A toy perimeter-defense problem with immobile attackers and defenders

We first discuss how cross-reactivity helps tackle heterogeneity using a toy problem where neither defenders nor attackers can “move”. Imagine that a fixed number of attackers spawn according to the attacker distribution Q_a and move with constant velocity towards a perimeter. Similarly, a fixed number of defenders spawn on the perimeter according to the defender distribution P_d . For a 1-dimensional perimeter defense problem, let us have the defenders be on the real line and they can only interact with attackers who seek to penetrate the line; see Fig. 1. The shape space here is the Euclidean location of the attackers and defenders. Defenders that are close to attackers are able to interact with the attacker with a higher probability and if the interaction succeeds, they can prevent harm. On the other hand, defenders that are very far away from the attacker have a small probability of successfully interacting with the attackers and are thus unable to stop the harm. The goal of the defense team is to place defenders along the perimeter and minimize the number of attackers that successfully penetrate the perimeter. This setting can be exactly captured by our model; the optimal defender distribution is shown in Fig. 1.

IV. MODELING MOBILE DEFENDERS

We now formulate the problem where defenders can move to different parts of a Euclidean state-space to intercept attackers. Again the coordinates $a, d \in \mathbb{R}$ are in Euclidean space. For the perimeter-defense setup, defenders *begin* at location d and can move on the real line with a speed u . Attackers arrive at a location a . Only the relative speed of the attackers and defenders matters, so we can set the speed of the attackers to be 1. Our key idea is to model the movement of the defenders using the cross-reactivity $f_{d,a,u}$. Consider the scenario where the intruder enters the field of view of the sensors of the defenders when it is 1 unit away from the

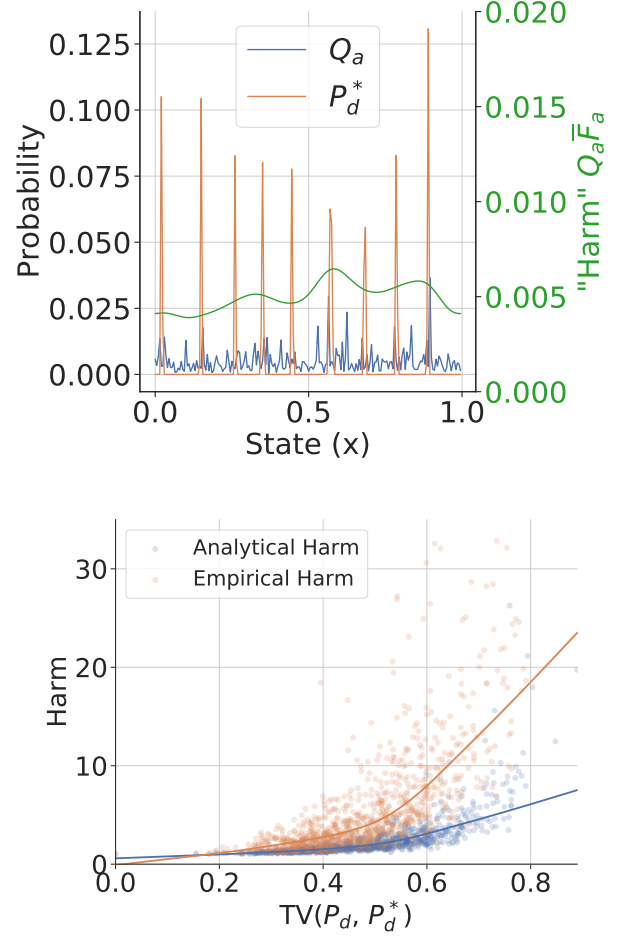


Fig. 1: Top: Defenders protect a perimeter $[0, 1]$ from attackers with distribution Q_a supported on $[0, 1]$. Probabilities Q_a are drawn from a log-normal distribution with coefficient of variation $\kappa^2 = \exp(\sigma_Q^2) - 1$ and normalized (blue). The optimal defender distribution P_d^* (orange) is found by optimizing (3). A cross-reactivity kernel $f_{d,a}$ of bandwidth $\sigma = 0.05$ leads to a discrete distribution that covers the state space. In green, we show the harm \bar{F}_a caused by attackers at different locations a weighted by their probability Q_a . This harm is relatively constant in spite of a discrete distribution P_d^* because of the cross-reactivity kernel $f_{d,a}$ with a non-zero bandwidth σ . The number of spikes in P_d^* will reduce for a larger σ and although the overall harm $\sum_a Q_a \bar{F}_a$ will increase, the harm by every attacker \bar{F}_a will be relatively constant.

Bottom: The harm incurred using a non-optimal P_d is close to that of the harm of P_d^* in Fig. 1 even for large differences, as measured in the total variation norm ($\frac{1}{2} \|P_d - P_d^*\|_1$). To obtain this plot, we sampled 1000 different P_d s (by perturbing the optimal P_d^* using log-normal noise) and computed the empirical and analytical harm against a fixed Q_a . This experiment also indicates that the empirical harm calculated using our experiments using (2) is close to the analytical harm (4) for a broad regime.

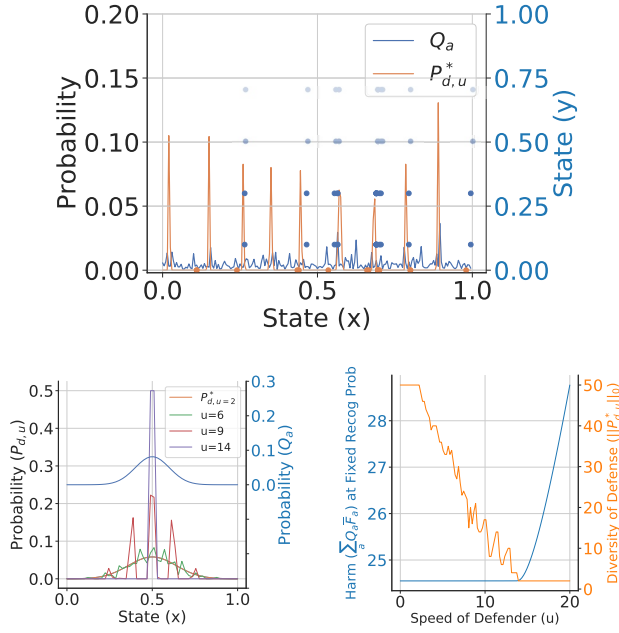


Fig. 2: Mobile defenders. Top: Attackers (blue dots) spawn at location $(a, 1)$ with $a \sim Q_a$ and move with constant speed towards the perimeter ($y = 0$). For each attacker, a defender (orange dot) spawns at initial state $(d(0), 0)$ with $d(0) \sim P_{d,u}^*$. At every step (indicated by progression of the blue dots, light to dark), defenders move along the perimeter towards their closest attacker with a speed u . Interaction between defender and attacker results in a recognition event if they are close ($|d(T) - a| < \epsilon$) at $T = 1$.

Bottom Left: For a simple attacker distribution Q_a (blue) with $\sigma_Q = 0.1$, we show $P_{d,u}^*$ for different speeds u and $\sigma = 0.01$. As discussed in §III, when the defender cross-reactivity bandwidth $\sigma_P = \sigma$ (or $\sigma_P = \sigma u$ for mobile defenders) is less than a threshold $\sigma_Q \sqrt{1 + \alpha}$, the optimal defender distribution is a Gaussian, otherwise it is a Dirac delta at the mean of the attacker distribution Q_a . For $\alpha = 1$ here, for speeds $u < 14$, the defender distribution is Gaussian, for higher speeds it is a Dirac delta distribution (purple).

Bottom Right: As the speed of defenders increases, we see two regimes for the tradeoff between diversity of defenders and the harm incurred by the defense. For small speeds, $u < 14$, while the shape of the distribution is still close to that of a Gaussian, the diversity of defenders starts reducing because the optimal defense need not maintain too many diverse defender types; the harm remains constant. At higher speeds, the diversity of the defenders reaches a minimum and stays constant while the harm (multiplied by a factor $(\sigma/\sigma_Q)^\alpha$ which ensures that we measure harm at constant recognition probability) increases by a small amount. The expression for the optimal defender distribution can be obtained as discussed in the Appendix; also see (D32)¹. This implies that for a fixed recognition probability, the optimal distribution $P_{d,u}^*$ reduces the number of different types of defenders if they have high mobility due to their larger cross-reactivity, at the cost of incurring a slightly higher harm.

perimeter. We set

$$f_{d,a,u} \propto e^{-(d-a)^2/(2u^2\sigma^2)} \quad (5)$$

If $u \ll (d-a)/(2\sigma)$, then the probability of interception is small and harm occurs. Our goal is to design the optimal distribution for the defenders $P_{d,u}^*$ that minimizes the harm caused by the attackers who cannot be intercepted. This setup can be solved using the same problem formulation as that of §II now by setting $\tilde{P}_a = \sum_{d,u} f_{d,a,u} P_{d,u}$. Fig. 2 discusses simulation experiments with mobile defenders.

V. ESTIMATING AN UNKNOWN ATTACKER DISTRIBUTION

Next we are interested in understanding settings where the attacker distribution Q_a is not known to the defenders and it may change over time. The attacker distribution can change in two ways, either there are different types of attackers that arrive as time progresses, or the attackers move in the state-space. We will discuss how to estimate $Q_a(t)$ and use this estimate to calculate a new optimal distribution for the defenders $P_d^*(t)$ at each time step. Interactions, both successful recognition events or unsuccessful ones, give observations of the attacker types a and thereby $Q_a(t)$.

Our model for how attackers proliferate enables us to estimate their distribution as follows. Let us first assume that Q_a is unknown to the defenders but it is stationary, i.e., it does not change with time. From §II, the expected number of attackers is $m_a(t)$ and it grows as $m_a(t) = m_a(0)e^{\nu_a t}$. Since we have $m_a(0) = 1$ for attackers a that were sampled from Q_a , if we can estimate $\hat{m}_a(0)$ then we can think of the attackers corresponding to it as sampled from Q_a and therefore obtain an estimate of Q_a .

Let us arrange all the attackers into a large vector $x(t) \in \mathbb{R}^{m_a(t)}$ which will be the state of the filter. We will assume that $x_i \sim N(\mu_i, \sigma_i)$ for $i \leq m_a(t)$; observations $y_i = cx_i + \xi$ where c is a Boolean that indicates if this specific attacker interacted with the defenders; $\xi \sim N(0, \sigma_\xi^2)$ is Gaussian noise. We can update $\mu_i^+ = \mu_i + k(y_i - c\mu_i)$ and $(\sigma_i^+)^2 = (1 - kc)\sigma_i^2$ using the Kalman gain $k = \sigma_i^2 c / (c^2 \sigma_i^2 + \sigma_\xi^2)$. The growth rate is estimated as $\hat{\nu}_i = \log(\mu_i^+ / \mu_i)$. Since there are multiple attackers for each type, we average the estimates as

$$\hat{\mu}_a(t) = \frac{\sum_{i=1}^{m_a(t)} \mathbf{1}_{\{\text{type}(x_i)=a\}} \mu_i}{\sum_{i=1}^{m_a(t)} \mathbf{1}_{\{\text{type}(x_i)=a\}}},$$

and similarly for $\hat{\nu}_a$ to get $\hat{Q}_a(t) = \hat{\mu}_a e^{-\hat{\nu}_a t}$. Let us emphasize that the number of attackers $m_a(t)$ (and therefore the dimensionality of the state x of the filter) growing with time is not an issue in the implementation. As discussed, the filter runs independently for each attacker (and therefore each attacker type) but is easy to incorporate a known model of the correlations between the growth rates ν_a of different attacker types. Given the estimate of $\hat{Q}_a(t)$, we recalculate the optimal defender distribution $P_d^*(t)$ by minimizing (3) at each instant. Fig. 3 discusses simulation experiments with a stationary Q_a .

The above expressions for $\hat{Q}_a(t)$ are derived for a stationary

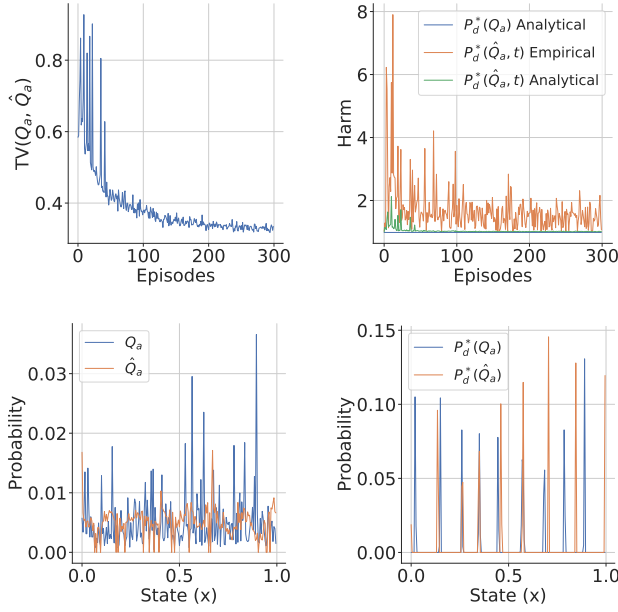


Fig. 3: Estimating an unknown and stationary attacker distribution. We initialize $\hat{Q}_a(0)$ to be uniform and set $P_d^*(0)$ using (3). The Kalman filter-based technique in §V is run for 300 episodes. At the beginning of each episode, we sample a new set of attackers from Q_a and within every episode $0 \leq t \leq T$, we sample defenders from $P_d^*(t)$ that is calculated on the basis of $\hat{Q}_a(t)$. The episode ends at a random time T when the last attacker is recognized by the defense and total harm of the episode is the harm incurred until all attackers are recognized. The estimate of \hat{Q}_a is initialized to its final value $\hat{Q}_a(T)$ from the previous episode. In other words, defenders get multiple opportunities to estimate the attacker distribution but *attacker types* can be different across episodes.

Top: The total-variation distance between the true Q_a and the estimated \hat{Q}_a decreases with the number of episodes (left). Remarkably, harm incurred by the defenders using the estimated \hat{Q}_a (green, (4)) converges to the optimal harm as if Q_a was known perfectly (blue) as the defenders see more episodes. The empirical harm (orange, (2)) is also close to the analytical harm (green). The large spikes in the right plot are due to noisy observations resulting from suboptimal defender distributions which further result in an inaccurate estimate of \hat{Q}_a . But once \hat{Q}_a stabilizes (around 100 episodes), the harm in subsequent episodes is at most twice the optimal.

Bottom: We show the final \hat{Q}_a estimated at the end of 300 episodes (orange) against the actual Q_a (blue) in the left plot. The corresponding defender distributions $P_d^*(\hat{Q}_a)$ (orange) and $P_d^*(Q_a)$ (blue) are shown on the right. Note that even if the estimation procedure does not recover the exact Q_a , the defender distribution for the estimated \hat{Q}_a is very similar to the defender distribution for the true Q_a , as is the harm in the top right plot. This indicates that in these highly stochastic problems with multiple agents (we have 1000 attackers and 1000 defenders) we can still meaningfully counter an unknown attacker distribution and obtain a defender distribution that incurs the optimal harm.

Q_a . If the attacker distribution is non-stationary and evolves with time, then we can still use the same expressions to estimate $\hat{Q}_a(0)$ but doing so will incur errors. But if the timescale of the evolution of Q_a is much slower than the growth rates ν_a and ν'_a (which determine how quickly the defenders interact and thereby tackle the attackers), then we can expect the estimate of $\hat{Q}_a(t)$ to converge faster than the evolution of $Q_a(t)$. In this paper, we do not focus on accurately tracking such evolving attacker distributions and instead use this simple trick. Fig. 4 discusses simulation experiments with a non-stationary Q_a .

VI. DECENTRALIZED CONTROL: COMPETITION BETWEEN DEFENDERS LEADS TO OPTIMAL RESOURCE ALLOCATION

The optimal defender distributions P_d^* or $P_{d,u}^*$ were calculated in a centralized fashion. In this section, we discuss how we can achieve optimal harm even if the control policy for the defenders, namely P_d^* is calculated in a decentralized fashion. The key idea is to exploit cross-reactivity between the defenders, i.e., the fact that multiple defenders can tackle the same attacker and set up competition among the defenders to earn the reward of successfully recognizing an attacker. Biology is similar, receptors that successfully recognize antigens proliferate at the cost of other receptors⁸.

Let the number of defenders of a particular type be N_d . We can set

$$\frac{dN_d}{dt} = N_d \left[\sum_a Q_a \varphi \left(\sum_{d'} N_{d'} f_{d',a} \right) f_{d,a} - c \right]. \quad (6)$$

Here, the constant c is the rate at which defenders d are decommissioned (the death rate in biology). In the first term, the total interaction of defender d with different attackers $\sum_a Q_a f_{d,a}$ is weighted by some function $\varphi(\cdot)$ which is a decreasing function of its argument. The quantity $\sum_{d'} N_{d'} f_{d',a}$ determines how many other defenders can tackle a . If this is large, then the incremental utility of having the specific defender d diminishes, and therefore its growth rate \dot{N}_d should be smaller. We will see in experiments that the harm caused by this decentralized dynamics converges to the optimal harm obtained from a centralized computation of P_d^* . We can also use the estimated attacker distribution \hat{Q}_a in place of the true distribution Q_a in (6) in situations where it is unknown to the defenders.

Fig. 5 shows an experiment with decentralized control when the attacker distribution Q_a is stationary while Fig. 6 shows a similar result when defenders estimate an evolving attacker distribution using the filter in §V. We have also obtained similar results for the case when defenders move and tackle a stationary attacker distribution (like that of §IV).

VII. DISCUSSION AND RELATED WORK

Pursuit-evasion games have seen a wide range of perspectives^{9,10}, surveys^{11,12}, and applications such as search and rescue¹³ and environmental monitoring¹⁴. Problems with multiple agents are complex due to their high dimensional

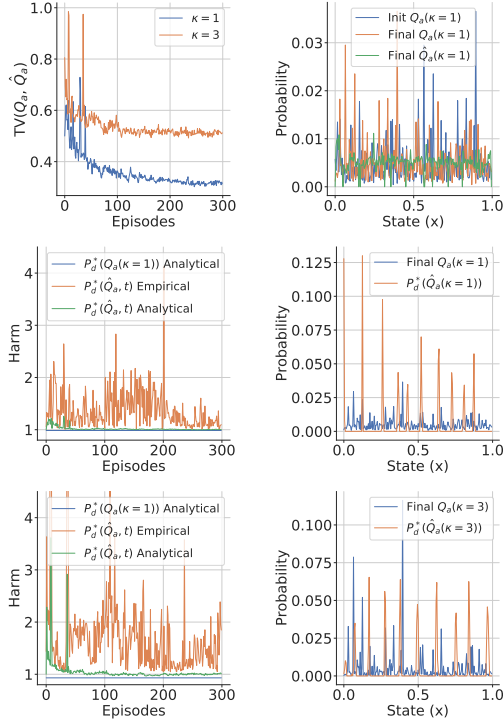


Fig. 4: Estimating a changing attacker distribution. For the same setting as that of Fig. 3, we run the filter when the attacker distribution shifts as $Q_{a+k} = Q_a$, i.e., after the k^{th} episode the probability of observing attacker $a+i$ is Q_a . The interval $[0, 1]$ is set to be isomorphic to $[0, 2\pi]$ in this case by setting $a = 0$ and $a = 1$ to be the same points. If the shape space consists of Euclidean locations of the agents, this models mobile attackers.

Top: Even if the estimation scheme is designed for a stationary Q_a , it can track an evolving attacker distribution (left). The initial ($k = 0$, blue) and final ($k = 300$, orange) attacker distributions Q_a for coefficient of variation $\kappa = 1$ and the final estimation \hat{Q}_a (green) at $k = 300$ (right). This shows that it is easier to estimate an evolving attacker distribution with a smaller κ .

Middle ($\kappa = 1$) and Bottom ($\kappa = 3$): We show the final Q_a (blue, right plots) and the estimated $P_d^*(\hat{Q}_a)$ (orange, right plots) for two situations, $\kappa = 1$ (middle) and $\kappa = 3$ (bottom). In both cases, the peaks of the the estimated P_d^* track the peaks of Q_a . The empirical harm incurred in this experiment (left, orange) converges to the analytical harm (left, green) and is close to optimal harm (left, blue) which is calculated using the true Q_a at each time step. The superior tracking for $\kappa = 1$ leads to lower variance in the empirical harm (middle left, orange) and a more biased P_d^* (middle right, orange) that is catered to the final $Q_a(\kappa = 1)$. In contrast, a poorer estimate of $\hat{Q}_a(\kappa = 3)$ (top left, orange) leads to a larger variance in the empirical harm (bottom left, orange). Note how the attacker distribution (blue, middle-bottom right) has more spikes for a larger κ . This experiment shows how cross-reactivity allows the defenders to both track and counter different types of attacker distributions.

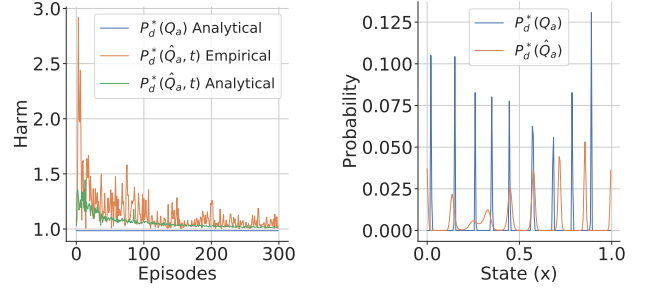


Fig. 5: Convergence to near-optimal harm using decentralized control. For the same setting as that of Fig. 3, we run the dynamics in (6) using the estimate $\hat{Q}_a(t)$ calculated using the Kalman filter to induce the optimal defender distribution $P_d^*(t)$ (instead of calculating it by minimizing the harm in (3) as done in Fig. 3). The harm in this case is slightly lower than that in Fig. 3, perhaps because of the transient dynamics in (6) which does not lead to P_d^* immediately but models the growth of defenders over time. We run the population dynamics for 10^6 iterations within each episode to obtain P_d^* . The defender distribution (orange, right) is again close to the optimal distribution P_d^* for Q_a but note that it is a bit smoother (and therefore sub-optimal). We know from Fig. 2 that there is a tradeoff between the diversity of the defender types (many types for a smooth distribution to few types for a spiked distribution) and harm (lower harm for the smooth distribution and higher harm for same recognition probability for the latter).

state-space¹⁵. We investigate a variant of the pursuit-evasion game first introduced as the target-guarding problem where the pursuer/defender tries to prevent the evader/intruder from reaching the target^{16,17}. A large body of the work on this problem^{18–20} studies how multiple defenders decompose the problem into smaller games^{21,22}, or reduce the defense strategy to an assignment problem²³.

A theme that has emerged recently in reinforcement learning-based multi-agent control^{24–26} is to obtain decentralized, cooperative policies^{27–29} to tackle non-stationarity and limited information. A popular paradigm is to train a centralized policy and execute it in a decentralized fashion^{30–34}. Emergence of coordination has also been studied^{35–37}. These methods typically suffer from poor sample complexity but some have been scaled to large problems using heuristics^{38–40}.

This work uses non-learned based methods but demonstrates scalable decentralized policies that can adapt to a wide range of changing attacker distributions for problems as large as 1000 attackers and defenders, albeit in the limited context of a perimeter-defense game. We also obtain a useful guiding principle: competition among the defenders where successful interaction with the attackers acts as the reward may achieve optimality of the resources spent. Such ideas can be used for designing new reinforcement learning methods for multi-agent control. Prior work has noticed the benefits of a similar competition arising out of stochastic policies⁴¹.

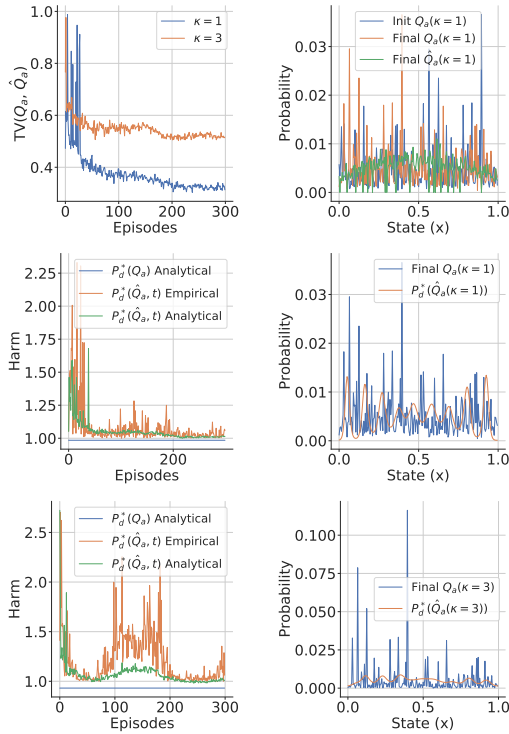


Fig. 6: Convergence to near-optimal harm using decentralized control for the case when the attacker distribution evolves across episodes. For the same setting as that of Fig. 4, i.e., when the attacker distribution shifts as $Q_{a+k} = Q_a$, we implemented the decentralized control dynamics using the estimate \hat{Q}_a obtained by the defenders. We have implemented a centralized estimation problem in this case, i.e., all defenders share information of their interactions with each other and thereby maintain a single estimate \hat{Q}_a .

Top: We show Q_a with coefficient of variation $\kappa = 3$ for the initial ($k = 0$) and final ($k = 300$) attacker distributions and the final estimation \hat{Q}_a at $k = 300$ (right). Like Fig. 4, the TV plot (left) shows that estimation of Q_a is easier for a smaller κ .

Middle ($\kappa = 1$) and Bottom ($\kappa = 3$): Like Fig. 5, the decentralized formulation gives rise to smooth defender distributions (orange, right). In the middle row, the distribution Q_a is less spiked and therefore the decentralized defender distribution is more spiked (and closer to the optimal one, as indicated by the empirical harm in orange vs. analytical harm in blue in the middle left plot). In the bottom row, the attacker distribution Q_a is more spiked which makes it more difficult to be estimated by the filter. Consequently, the defender population induced by the decentralized dynamics is also sub-optimal (orange in bottom right is farther away from optimal, as indicated by the empirical harm in orange being farther away from the optimal harm in blue in the bottom left plot). The empirical harm for $\kappa = 3$ again has a higher variance than that of the middle row. This experiment indicates that the decentralized population dynamics in (6) is capable of both tracking and countering an evolving attacker distribution.

Our work is inspired from how the adaptive immune system in humans is organized. We strongly build upon the recent literature in biophysics which models the response of the adaptive immune system in an environment with a large number of evolving pathogens^{42–44}. We believe that the salient traits exhibited in the immune system such as heterogeneous defender types with wide cross-reactivity that interact with a range of attackers, and decentralized estimation and execution are key building blocks for understanding multi-agent autonomy. There are also a number of works that use bio-inspired approaches mimicking the behavior of ants, bees and flocks^{45–47} for multi-agent control.

Broadly speaking, *modeling* heterogeneity has received relatively little interest⁴⁸. Heterogeneity comes in many forms such as differences in roles^{49–51}, robotic capabilities and or sensors^{52,53}, dynamics^{54,55}, and even teams of air and ground robots^{56,57}. But algorithmic methods that can tackle large-scale heterogeneity have been difficult to build. This work uses a simple formulation to understand how to devote resources optimally in a heterogeneous environment.

REFERENCES

- [1] Mayer, A., Balasubramanian, V., Mora, T. & Walczak, A. M. How a well-adapted immune system is organized. *PNAS* **112**, 5950–5955 (2015).
- [2] Perelson, A. S. & Oster, G. F. Theoretical studies of clonal selection: Minimal antibody repertoire size and reliability of self-non-self discrimination. *Journal of Theoretical Biology* **81**, 645–670 (1979).
- [3] Smith, J. G. The information capacity of amplitude-and variance-constrained scalar Gaussian channels. *Information and control* **18**, 203–219 (1971).
- [4] Laughlin, S. A simple coding procedure enhances a neuron’s information capacity. *Zeitschrift für Naturforschung c* **36**, 910–912 (1981).
- [5] Berger, J. O., Bernardo, J. M. & Sun, D. The formal definition of reference priors. *The Annals of Statistics* **37**, 905–938 (2009).
- [6] Mattingly, H. H., Transtrum, M. K., Abbott, M. C. & Machta, B. B. Maximizing the information learned from finite data selects a simple model. *PNAS* **115**, 1760–1765 (2018).
- [7] Gao, Y., Ramesh, R. & Chaudhari, P. Deep reference priors: What is the best way to pretrain a model? *ICML* (2022).
- [8] De Boer, R. J. & Perelson, A. S. T cell repertoires and competitive exclusion. *Journal of Theoretical Biology* **169**, 375–390 (1994).
- [9] Karaman, S. & Frazzoli, E. Incremental sampling-based algorithms for a class of pursuit-evasion games. vol. 68, 71–87 (2010).
- [10] Isaacs, R. *Differential Games I: Introduction* (RAND Corporation, 1954).
- [11] Chung, T., Hollinger, G. & Isler, V. Search and pursuit-evasion in mobile robotics. *Auton. Robots* **31** (2011).
- [12] Robin, C. & Lacroix, S. Multi-robot Target Detection and Tracking: Taxonomy and Survey. *Autonomous Robots* **40**, pp.729–760 (2016).
- [13] Kumar, V., Rus, D. & Singh, S. Robot and sensor networks for first responders. *IEEE Pervasive Computing* **3**, 24–33 (2004).
- [14] Dunbabin, M. & Marques, L. Robots for environmental monitoring: Significant advancements and applications. *RAM* **19**, 24–39 (2012).
- [15] Hilal, A. R. An intelligent sensor management framework for pervasive surveillance (2013).
- [16] Garcia, E., Casbeer, D. W., Pham, K. & Pachter, M. Cooperative aircraft defense from an attacking missile. In *CDC*, 2926–2931 (2014).
- [17] Shishika, D. & Kumar, V. A review of multi agent perimeter defense games. In *Decision and Game Theory for Security*, 472–485 (2020).
- [18] Shishika, D., Paulos, J. & Kumar, V. Cooperative team strategies for multi-player perimeter-defense games. *RAL* **5**, 2738–2745 (2020).
- [19] Von Moll, A., Shishika, D., Fuchs, Z. & Dorothy, M. The turret-runner-penetrator differential game. In *ACC*, 3202–3209 (2021).
- [20] Lee, E. S., Shishika, D., Loianno, G. & Kumar, V. Defending a perimeter from a ground intruder using an aerial defender: Theory and practice. In *SSRR*, 184–189 (2021).

- [21] Shishika, D. & Kumar, V. Local-game decomposition for multiplayer perimeter-defense problem. 2093–2100 (2018).
- [22] Macharet, D., Chen, A., Shishika, D., Pappas, G. & Kumar, V. Adaptive partitioning for coordinated multi-agent perimeter defense. In *IROS*, 7971–7977 (2020).
- [23] Chen, M., Zhou, Z. & Tomlin, C. J. A path defense approach to the multiplayer reach-avoid game. In *CDC*, 2420–2426 (2014).
- [24] Tan, M. Multi-agent reinforcement learning: Independent vs. cooperative agents. In *ICML*, 330–337 (1993).
- [25] Lowe, R. *et al.* Multi-agent actor-critic for mixed cooperative-competitive environments. arXiv 1706.02275 (2020).
- [26] Jeong, H., Hassani, H., Morari, M., Lee, D. D. & Pappas, G. J. Learning to track dynamic targets in partially known environments. arXiv 2006.10190 (2020).
- [27] Adler, M., Racke, H., Sivasadan, N., Sohler, C. & Vocking, B. Randomized pursuit-evasion in graphs. In *Automata, Languages and Programming*, 901–912 (2002).
- [28] Khan, A., Tolstaya, E., Ribeiro, A. & Kumar, V. Graph policy gradients for large scale robot control. arXiv 1907.03822 (2019).
- [29] Li, S., Gupta, J. K., Morales, P., Allen, R. & Kochenderfer, M. J. Deep implicit coordination graphs for multi-agent reinforcement learning. arXiv 2006.11438 (2021).
- [30] Wang, Y., Dong, L. & Sun, C. Cooperative control for multi-player pursuit-evasion games with reinforcement learning. *Neurocomputing* **412**, 101 – 114 (2020).
- [31] Son, K., Kim, D., Kang, W. J., Hostallero, D. E. & Yi, Y. Qtran: Learning to factorize with transformation for cooperative multi-agent reinforcement learning. arXiv 1905.05408 (2019).
- [32] Foerster, J., Farquhar, G., Afouras, T., Nardelli, N. & Whiteson, S. Counterfactual multi-agent policy gradients. arXiv 1705.08926 (2017).
- [33] Sharma, P. K., Zaroukian, E., Fernandez, R., Basak, A. & Asher, D. E. Survey of recent multi-agent reinforcement learning algorithms utilizing centralized training. In *AI and ML for Multi-Domain Operations Applications III*, vol. 11746, 117462K (2021).
- [34] Terry, J. K., Grammel, N., Hari, A., Santos, L. & Black, B. Revisiting parameter sharing in multi-agent deep reinforcement learning. arXiv 2005.13625 (2020).
- [35] Barton, S. L., Zaroukian, E., Asher, D. E. & Waytowich, N. R. Evaluating the coordination of agents in multi-agent reinforcement learning. In *International Conference on Intelligent Human Systems Integration*, 765–770 (2019).
- [36] Asher, D. E. *et al.* Multi-agent collaboration with ergodic spatial distributions. In *Artificial Intelligence and Machine Learning for Multi-Domain Operations Applications II*, vol. 11413, 114131N (2020).
- [37] Baker, B. *et al.* Emergent tool use from multi-agent autocurricula. arXiv 1909.07528 (2020).
- [38] Khan, A., Zhang, C., Lee, D. D., Kumar, V. & Ribeiro, A. Scalable centralized deep multi-agent reinforcement learning via policy gradients. 1805.08776 (2018).
- [39] Low, K. H., Leow, W. K. & Ang, M. H. Autonomic mobile sensor network with self-coordinated task allocation and execution. *IEEE Transactions on Systems, Man, and Cybernetics* **36**, 315–327 (2005).
- [40] Long, Q. *et al.* Evolutionary population curriculum for scaling multi-agent reinforcement learning. arXiv 2003.10423 (2020).
- [41] Hsu, C. D., Jeong, H., Pappas, G. J. & Chaudhari, P. Scalable reinforcement learning policies for multi-agent control. In *IROS*, 4785–4791 (2020).
- [42] Mayer, A., Balasubramanian, V., Walczak, A. M. & Mora, T. How a well-adapting immune system remembers. *PNAS* **116**, 8815–8823 (2019).
- [43] Mayer, A., Mora, T., Rivoire, O. & Walczak, A. M. Diversity of immune strategies explained by adaptation to pathogen statistics. *PNAS* **113**, 8630–8635 (2016).
- [44] Mayer, A., Zhang, Y., Perelson, A. S. & Wingreen, N. S. Regulation of t cell expansion by antigen presentation dynamics. *PNAS* **116**, 5914–5919 (2019).
- [45] Hsieh, M. A., Halasz, . M., Berman, S. & Kumar, V. R. Biologically inspired redistribution of a swarm of robots among multiple sites. *Swarm Intelligence* **2**, 121–141 (2008).
- [46] Franks, N., Pratt, S., Mallon, E., Britton, N. & Sumpter, D. Information flow, opinion polling and collective intelligence in house-hunting social insects. *Philosophical transactions of the Royal Society of London. Series B, Biological sciences* **357**, 1567–83 (2002).
- [47] Zavlanos, M. M., Tanner, H. G., Jadbabaie, A. & Pappas, G. J. Hybrid control for connectivity preserving flocking. *TAC* **54**, 2869–2875 (2009).
- [48] Mitra, A., Hassani, H. & Pappas, G. Exploiting heterogeneity in robust federated best-arm identification. arXiv 2109.05700 (2021).
- [49] Fernandez, R. *et al.* Emergent heterogeneous strategies from homogeneous capabilities in multi-agent systems. In *Advances in Artificial Intelligence and Applied Cognitive Computing*, 491–498 (2021).
- [50] Wang, T., Dong, H., Lesser, V. & Zhang, C. Roma: Multi-agent reinforcement learning with emergent roles. arXiv 2003.08039 (2020).
- [51] Wang, T. *et al.* Rode: Learning roles to decompose multi-agent tasks. arXiv 2010.01523 (2020).
- [52] Salam, T. & Hsieh, M. A. Heterogeneous robot teams for modeling and prediction of multiscale environmental processes. arXiv 2103.10383 (2021).
- [53] Shishika, D., Paulos, J., Dorothy, M. R., Ani Hsieh, M. & Kumar, V. Team composition for perimeter defense with patrollers and defenders. In *CDC*, 7325–7332 (2019).
- [54] Szwajkowska, K. *et al.* Collective motion patterns of swarms with delay coupling: Theory and experiment. *Phys. Rev. E* **93**, 032307 (2016).
- [55] Edwards, V., Rezeck, P., Chaimowicz, L. & Hsieh, M. A. Segregation of Heterogeneous Robotics Swarms via Convex Optimization. Dynamic Systems and Control Conference (2016).
- [56] Chaimowicz, L. *et al.* Deploying air-ground multi-robot teams in urban environments. In *Multi-Robot Systems. From Swarms to Intelligent Automata Volume III*, 223–234 (2005).
- [57] Grocholsky, B., Keller, J., Kumar, V. & Pappas, G. Cooperative air and ground surveillance. *RAM* **13**, 16–25 (2006).

VIII. APPENDIX

The optimal defender distribution P_d^* is found by minimizing (3) with respect to P_d , subject to constraints of non-negativity ($P_d \geq 0$) and normalization ($\sum_d P_d = 1$). We can define an augmented Lagrangian as

$$L = \sum_a Q_a \bar{F}_a + \lambda \left(\sum_d P_d - 1 \right) - \sum_d \nu_d P_d$$

where λ and ν_d are Lagrange multipliers and set its derivative to zero to get the optimality conditions

$$\sum_a Q_a \tilde{P}_a^{-\alpha} \Gamma(1 + \alpha) = -\lambda^* + \nu_d^*$$

$$\nu_d^* \geq 0 \quad (\text{dual feasibility})$$

$$\nu_d^* P_d^* = 0 \quad (\text{complementary slackness})$$

If $P_d^* > 0$ for some d , we have $\nu_d^* = 0$ and thus $\sum_a Q_a \tilde{P}_a^{-\alpha} \Gamma(1 + \alpha) = -\lambda^*$. We can solve these equations for specific choices of cross-reactivity $f_{d,a}$ ¹.

If the shape-space is continuous and the cross-reactivity is $f_{d,a} = f(d - a)$, then we can write the first condition as

$$\int da Q_a \bar{F}'(\tilde{P}_a^*) f(d - a) = -\lambda^*$$

where the total probability of tackling attacker a is again a convolution $\tilde{P}_a^* = \int dd P_d f(d - a)$. We can now solve for \tilde{P}_a^* by noticing that $Q_a \bar{F}'(\tilde{P}_a^*) f(d - a) = -c$ satisfies this equation for some constant c (the convolution of a constant is a constant). Given such a \tilde{P}^* we can calculate the optimal defender distribution as

$$P_d^* = \mathcal{F}^{-1}[\mathcal{F}[\tilde{P}^*]/\mathcal{F}[f]].$$

where $\mathcal{F}[\cdot]$ denotes the Fourier transform¹.